4

This thesis

"Se non ora, quando?"
—Primo Levi

4.1 RESEARCH CONTEXT AND DESCRIPTION

The interplay between interstellar dust, ice and gas plays a key role in the journey starting in dense molecular clouds and ending with the rise of new planetary systems. Along this path, ice mantles on dust grains can be described as open systems, in constant exchange with the surrounding gas phase through accretion and desorption processes. The outcome of this mutual ice-gas interaction are organic molecules of different levels of complexity (Jørgensen *et al.*, 2020). These can evolve into biomolecules and undergo an intricate and poorly understood cascade of biochemical reactions, which ultimately can give rise to living organisms in the Universe. In this context, a logical approach to constrain the formation of complex molecules consists of investigating the chemical processes during the formation of solar-type stars. In other words, providing constraints on the nature of the material and the relative importance of the mechanisms involved in the gas and ice interplay during stellar evolution.

At present, a lot is still unknown about the degree of chemical complexity and the relationships between the intertwined solid-state and gas-phase chemistries in stellar nurseries. The count of securely detected molecules in the ISM (> 200) increased considerably in the last decades and with it, the existence of new chemical routes in star-forming regions (McGuire, 2018). However, despite the recent advances in the field, some ultimate questions remain unanswered such as:

- What are the exact processes linking solid-state and gas-phase species in cold protostellar envelopes?
- To what degree the physical environment impacts the solid- and gas-phase chemistries during the formation of low-mass protostars?

To address the above questions, in this thesis I carried out multi-wavelength observational studies of low-mass protostellar envelopes using a suite of millimeter and infrared facilities (e.g., the *Submillimeter Array* (SMA), *the Atacama Pathfinder EXperiment* (APEX), the *Institut de RadioAstronomie Millimétrique* (IRAM) 30m, the *James Clerk Maxwell Telescope* (JCMT), and the *Very Large Telescope* (VLT)). To access whether the physical conditions affect the gas and ice interplay, the selected sample consists of young stellar objects

located in three nearby star-forming regions, which do not share similar formation histories and are characterized by different physical structures. The targeted regions, the Serpens SVS4 cluster in Serpens Main, the multi-protostellar system IRAS 05417+0907 in the λ Orionis Barnard 35A cloud, and the Coronet cluster in Corona Australis are described in Chapter 3.

The approach followed consists of combining millimeter and near-/mid-infrared observations, and thus directly obtain and compare abundances of key astrochemical molecules, particularly of methanol, in both solid and gas phases towards the same astrophysical region. This procedure, previously adopted by Öberg *et al.* (2009a) and Noble *et al.* (2017), provides critical information tracing the solid-state and gas-phase chemistries in a complementary manner. In other words, it makes it possible to relate small-scale variations in the ice chemistry probed by infrared observations with large-scale astrophysical phenomena explored with millimeter observations.

Comparative studies similar to the ones presented in Chapters 5, 6, and 7 are relatively uncommon due to the challenges in obtaining observational constraints on solid-state chemistry. This is primarily due to the difficulties in disentangling the contribution of multiple molecules from blended absorption bands (Sect. 2.2) and to the low sensitivity of infrared observations, which hampers the detection of solid-state molecules with abundances with respect to H_2 below $\approx 10^{-6} - 10^{-7}$. In comparison, millimeter observations can detect gas-phase molecules with fractional abundances as low as $\approx 10^{-12}$. Additionally, the sample of sources for which spectroscopic infrared data exist is significantly reduced compared to the regions for which millimeter data are available (Boogert *et al.*, 2015). This reflects the fact that the observation of several ice bands is only possible from space as described in Chapter 2. As a consequence of the above, solid-state and gas-phase observations are frequently treated separately or the latter are often invoked to indirectly constrain solid-state chemistry. However, this approach leads to severe assumptions on the composition of the ice mantles, on the grain-surface chemistry and on how efficiently molecules are desorbed to the gas-phase (Noble *et al.*, 2017). One way to observationally overcome these assumptions is to compare, whenever possible, direct measurements of solid-state and gas-phase molecules.

To determine the abundances of gas-phase molecules and of their solid counterparts, and to cast light onto the poorly constrained non-thermal desorption processes described in Chapter 1, the most appropriate targets are the coldest shielded regions of protostellar envelopes, where the ice mantles are not thermally desorbed and, by consequence, non-thermal desorption processes are the most dominant (Sect. 1.3). To map the emission towards these extended regions at rather high-angular resolution ($3 - 4''$), the adopted observation strategy consisted of accompany interferometric observations with single-dish observations (Sect. 2.3.4). This procedure allows to recover the extended emission filtered out by the interferometer and to perform a quantitative analysis of the observational data.

The most suitable molecule for this type of comparative studies is methanol for multiple reasons. First, it is the only complex organic molecule unambiguously detected in both solid and gas phases. Interestingly, it is the simplest among the COMs detected in the gas-phase (McGuire, 2018), but

it is the most complex molecule securely detected in the ice mantles in interstellar and circumstellar environments (Boogert *et al.*, 2015). Second, CH_3OH is primarily formed in the solid-state (Watanabe and Kouchi, 2002; Fuchs *et al.*, 2009), as its gas-phase formation pathways are considered to be remarkably less efficient in comparison (Roberts and Millar, 2000; Garrod and Herbst, 2006; Geppert *et al.*, 2006). This indicates that CH_3OH is the ideal species to constrain non-thermal desorption mechanisms. Consequently, in the past years laboratory experiments and models have focused on determining non-thermal desorption rates and efficiencies principally for methanol with respect to other interstellar species (e.g., Öberg *et al.*, 2009b; Bertin *et al.*, 2016; Cruz-Diaz *et al.*, 2016; Martín-Doménech *et al.*, 2016; Minissale *et al.*, 2016a; Cazaux *et al.*, 2016). As a result, one of the aims of this thesis is to provide observational constraints to the current laboratory and computational predictions.

Finally, methanol is considered to be the "seed" molecule for the production of complex organic species both in the solid-state (e.g., Öberg *et al.*, 2009b; Chuang *et al.*, 2016; Fedoseev *et al.*, 2017) and in the gas gas-phase (e.g., Shannon *et al.*, 2014; Balucani *et al.*, 2015; Vazart *et al.*, 2020). This implies that current astrochemical models largely rely on the presence of CH_3OH ice and its efficient desorption to explain the observed abundances of complex organics in the hot-corino stage and in the cold phase. However, in some cases this can lead to overestimated gas-phase CH_3OH abundances compared to the observed values (e.g., Vasyunin and Herbst, 2013; Vasyunin *et al.*, 2017). This reflects the poorly known values for non-thermal desorption efficiencies and the overall challenges in providing observational constraints on CH_3OH ice in star-forming regions (Boogert *et al.*, 2015). Alternatively, there might be other chemical routes to unveil which link solid-state and gas-phase CH_3OH to the production of COMs in star-forming regions.

4.2 PUBLICATIONS

This section provides a summary overview of the scientific articles included in Chapters 5, 6, 7. The articles are:

1. G. Perotti, W. R. M. Rocha, J. K. Jørgensen, L. E. Kristensen, H. J. Fraser, and K. M. Pontoppidan 2020, A&A, 643, A48. "Linking ice and gas in the Serpens low-mass star-forming region";

2. G. Perotti, J. K. Jørgensen, H. J. Fraser, A.N. Suutarinen, L. E. Kristensen, W. R. M. Rocha, P. Bjerkeli, K. M. Pontoppidan, 2021, A&A, 650, A168. "Linking ice and gas in the λ Orionis Barnard 35A cloud";

3. G. Perotti, J. K. Jørgensen, L. E. Kristensen, W. R. M. Rocha, E. Artur de la Villarmois, H. J. Fraser, P. Bjerkeli, M. Sewilo, S. B. Charnley, in preparation. "Linking ice and gas in the Coronet cluster in Corona Australis". The inclusion of the awarded second track of SMA data is required to complete this article. This observational run has been delayed due to the shutdown of the SMA due to Covid-19.

4.2.1 *Article I: Linking ice and gas in the Serpens low-mass star-forming region*

This paper presents a study the gas-ice interplay towards ten deeply embedded low-to-intermediate mass protostars constituting the Serpens SVS4 cluster in Serpens Main (Sect. 3.1). In particular, millimeter and near-infrared observations are combined to obtain direct measurements of CH_3OH and CO gas-phase and ice towards the ten young protostars. The SMA and APEX datasets are folded together to recover the spatially extended emission filtered out by the interferometer in the manner described in Sect. 2.3.4. Simultaneously, the VLT-ISAAC near-infrared data are decomposed using a combination of laboratory components and analytical functions using the OMNIFIT fitting utility (Sect. 2.2.1). Finally, the chemical behaviours of these two pivotal gas-phase species are analysed and directly compared to their ice counterparts. To maintain the ice and gas measurements in their own reference frame, two separate H_2 column density maps are derived: one from SCUBA−2 submillimeter continuum maps at 850 μm, and one from the extinction in the J-band to adopt in the abundance determination of the gas-phase and ice species, respectively.

An important conclusion of this observational study is that the gas and ice variations towards the Serpens SVS4 cluster members do not show clear trends. This lack of correlation is attributed to the complex physical structure of the SVS4 cluster, plausibly embedded in the protostellar envelope of the Class 0 protostar SMM4 and affected by the outflow associated with this young source. This indicates that care should be taken when assuming the abundance of solid-state species from known gas-phase abundances and vice versa. Another important result is that the calculated CH_3OH gas-to-ice ratios in the cluster range from 1.4×10^{-4} to 3.7×10^{-3}. The sources responsible for the lower values of the CH_3OH gas-to-ice ratio are either the most deeply embedded or the ones located further away from the main source of UV irradiation, the Class 0 SMM4, where the non-thermal desorption of CH_3OH ice is less efficient. The lower values of the CH_3OH gas-to-ice ratios are in good agreement with the observational study by Öberg *et al.* (2009a) reporting a CH_3OH gas-to-ice ratio equal to 1.2×10^{-4} and to the astrochemical predictions by Cazaux *et al.* (2016).

4.2.2 *Article II: Linking ice and gas in the λ Orionis Barnard 35A cloud*

The main focus of this article is the gas-ice interplay towards the multi-protostellar system IRAS 05417+0907 in the λ Orionis Barnard 35A (B35A) cloud. This system is composed by at least four sources: B35A−2, B35A−3, B35A−4, B35A−5. Compared to Serpens Main, this region is impacted by the stellar winds from the nearby high-mass star λ Orionis, which is thought to be responsible for the star-formation activity in B35A (Sect. 3.2). Therefore, one of the main aims of this paper is to analyse the dependencies of the gas-ice interaction of a second nearby star-forming region, characterized by a physical environment which diverges from Serpens SVS4. We adopt the same observational strategy used in *Article I*: the SMA and APEX datasets are combined to recover the extended CH_3OH emission, whereas SMA and archival IRAM 30m data are folded together to account for the missing CO isotopologues emission. Archival ice column densities determined from

AKARI observations of IRAS 05417+0907 are used to compare the gas and ice abundances.

Our observations show that CH_3OH probes the trajectory of the giant outflow emanated from IRAS 05417+0907, and that the observed CH_3OH emission is due to non-thermal desorption mechanisms, plausibly sputtering of CH_3OH ice during shock events. One important consideration is that none of the targeted species shows an expected trend in ice abundances with respect to gas-abundances, corroborating the result obtained in *Article I*, and suggesting that the interaction between ice and gas species is more complex than previously thought. A second important conclusion is that the dust column density probed by the submillimeter emission is not directly linked to the H_2O ice column density. For instance, the H_2O ice column density is higher towards the protostellar object B35A−4 compared to object B35A−5, whereas the opposite is seen for the submillimeter dust emission. Our conclusion is that this discrepancy is due to the fact that B35A−5 is located along the trajectory of the outflow terminating in the Herbig-Haro object HH 175, in a region where sputtering and heating impact the morphology of the observed submillimeter dust emission. This study shows that millimeter and near-infrared observations are complementary and indispensable to relate the small-scale variations of grain-surface and ice chemistry with large-scale astrophysical phenomena traced by millimeter observations.

4.2.3 *Article III: Linking ice and gas in the Coronet cluster in Corona Australis*

In this article, we focus on the gas-ice interplay towards a third nearby star-forming region, the Coronet situated in Corona Australis (Sect. 3.3). Although it is a deeply embedded cluster of young stellar objects resembling Serpens SVS4, the Coronet harbours a younger stellar population which is strongly irradiated by the nearby Herbig Ae/Be star R CrA. Therefore, this region is an ideal testbed to study the effects of external irradiation from Herbig Ae/Be stars onto the ice and gas chemistries in low-mass protostellar envelopes. The SMA observations are used to study the gas-phase molecular inventory, whereas archival SMA, APEX, and Spitzer Space Telescope data are used to determine the CH_3OH gas-to-ice ratios in the region.

A first important conclusion is that the gas-phase chemistry of the Coronet is affected by the high UV flux from the nearby R CrA. This is reflected in the enhanced emission of formaldehyde (H_2CO) not associated with the young stellar objects in the field of view. In contrast, the H_2CO emission is confined to two ridges which show peculiar shapes, supporting the idea of Lindberg and Jørgensen (2012) that the cluster is strongly impacted by external heating. Additionally, the detection of molecular tracers of shocks such as sulfur oxides (SO, SO_2) at the locations of IRS7A and SMM1C, and of silicon oxide (SiO) south of R CrA suggests that IRS7A, SMM1C and R CrA are likely responsible for outflows and Herbig-Haro objects in the region.

Another important consideration is obtained from the analysis of the gas and ice variations in the Coronet. The comparison reveals a negative trend between the ammonium ion (NH_4^+) and H_2CO gas abundances, with the caveat that NH_4^+ is one of the carriers of the 6.85 μm band. This result indicates that the high-temperature regions traced by the emission of H_2CO

have a lower content of NH_4^+ residing on the grains, in agreement with its desorption with increasing dust temperatures. Finally, the CH_3OH gas-to-ice ratios calculated towards the Coronet from literature data are consistent with the values obtained in *Article I*.

4.3 OVERALL CONCLUSIONS AND OUTLOOK

Taken together, the main contributions of the dissertation research to the field are:

- There is not a one-to-one correspondence between the abundance of gas-phase species and their ice counterparts. As a matter of fact, ice and gas variations towards the studied regions do not follow a predictable trend. This implies that invoking ice chemistry and grain-surface chemistry to explain the observed gas-phase abundances can lead to inaccurate results, especially without an extensive knowledge of the physical environment surrounding the sources of interest.

- The CH_3OH gas-to-ice ratios constrained from observations validate the predicted values ($\sim 10^{-3} - 10^{-4}$) proposed by laboratory experiments (e.g., Öberg *et al.*, 2009b) and models (e.g., Cazaux *et al.*, 2016), favouring an efficient non-thermal desorption of methanol in the gas-phase of cold envelopes. This observational constraint accounts for multiple non-thermal desorption mechanisms, and not for methanol photodesorption only.

- The distribution of CH_3OH gas-to-ice ratios for the Coronet, Serpens SVS4, and towards low-mass Class 0/I protostars in Öberg *et al.* (2009a) suggests that the CH_3OH chemistry at play in cold low-mass protostellar envelopes, located in different low-mass star-forming regions is rather insensitive to varying physical conditions as can be seen in Figure 4.1. However, a larger sample of CH_3OH gas-to-ice ratios is needed to provide a conclusive assessment.

- The combination of infrared and millimeter observations is fundamental to cast light onto the gas-ice interplay, and hence to link the small-scale variations in the ice chemistry with large-scale astrophysical phenomena probed by millimeter observations.

With the awareness of the importance of the gas and ice interplay in the production of complex molecules, it has become clear that gas-phase and solid-state observations are complementary and that their concurrent analysis can advance our understanding of key aspects of star- and planet formation (e.g., desorption processes and snow-lines). Future infrared facilities, most notably the *James Webb Space Telescope* (JWST), will provide high-sensitivity maps of interstellar ice molecules in a variety of astrophysical environments. Compared to its predecessor, the *Spitzer Space Telescope*, the sensitivity of JWST will be fifty times higher at 7 μm just because of its sheer collecting area. Therefore, JWST observations will make it possible to provide better constraints on the solid-state abundances of the eight species securely detected in the ice mantles (H_2O, CO, CO_2, NH_3, CH_4, CH_3OH,

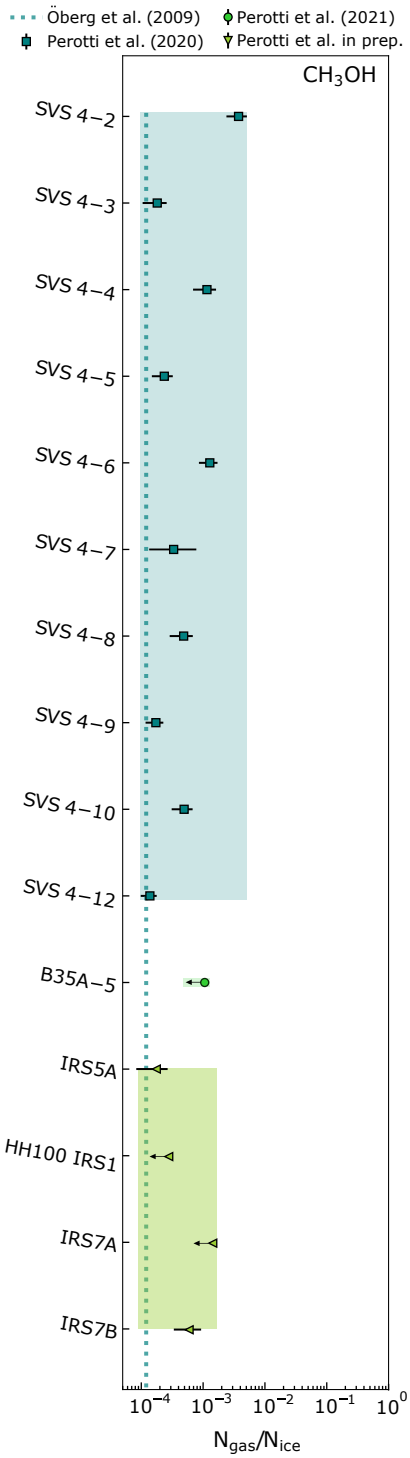

FIGURE 4.1: CH_3OH gas-to-ice ratios (N_{gas}/N_{ice}) towards low-mass protostars in Serpens SVS 4, Orion B35A and Coronet. The Serpens SVS 4 ratios (dark green squares) are from Perotti *et al.* (2020), whereas the Orion B35A upper limit (light green circle) is from Perotti *et al.* (2021). The light green triangles indicate the ratios estimated in Perotti et al. in preparation for the Coronet cluster in Corona Australis. The dotted light blue line marks the averaged CH_3OH gas-to-ice ratio determined for Class 0/I objects in Öberg *et al.* (2009a). The shaded areas indicate the ranges of gas-to-ice ratios towards the three molecular clouds.

^{13}CO and $^{13}CO_2$) and to confirm the tentative detections (e.g., NH_4^+, H_2CO, HCOOH, CH_3CHO, CH_3CH_2OH).

In this respect, an obvious continuation of the work presented in this thesis will be the combination of high-sensitivity ALMA and JWST data. The ice and gas interplay will be explored systematically for each evolutionary stage of the star-formation process, from cold clouds to nearby edge-on protoplanetary disks. These observational constraints will make it possible to trace the chemical journey of the material from the clouds to the planet-forming zone, and hence to understand what is the level of chemical complexity of the matter incorporated into comets and planets. The outcomes of these studies can be compared to the composition of cometary material or of the organic matter found in pristine records of the early Solar System, carbonaceous chondrites. The dependency of the gas-to-ice ratios, and therefore of the interconnected gas-phase and ice chemistries on the physical conditions will be addressed routinely for multiple interstellar species, eventually more complex than CH_3OH (e.g., CH_3CH_2OH). Particularly important for this purpose will be the comparison between the gas-to-ice ratios obtained towards clusters of young stellar objects versus isolated protostars, to disentangle the relative importance of different astrophysical phenomena.

The resulting observational constraints will motivate compelling laboratory experiments, especially of non-thermal desorption processes. At present, the most studied non-thermal desorption channel in the laboratory is photo-desorption, but even for this process, the rates and yields have only be determined for a handful of interstellar ice molecules. The yields of the other non-thermal desorption mechanisms described in Sect. 1.2.3 are unknown for the majority of the interstellar species. Consequently, astrochemical models often do not include non-thermal desorption processes or only for a limited number of species, which in turn affects the model results. It is therefore a priority to obtain reliable laboratory and model predictions to confront with observational results. In particular, it is of paramount importance to increment modelling efforts simulating the ice photo-chemistry of methanol and of more complex organics under laboratory conditions, to gain a better understanding of the reactions which regulate the ice chemistry prior and during the core collapse.

Another important venue for future work will be comparative studies of the observationally constrained gas-to-ice ratios with the values obtained from radiative transfer models combined with astrochemical models, specifically tuned to reproduce the physical structure of the targeted objects. These will be of uttermost importance for the study of the gas-ice interplay in protoplanetary disks, to determine at which radii from the central protostar specific molecules are thermally desorbed (i.e., the location of snow-lines) and how this affects the chemical composition of the forming planets.

4.4 OWN CONTRIBUTIONS VERSUS CONTRIBUTIONS OF COLLABORATORS

This section reports my own contributions to the articles and the contributions of my collaborators.

Article I This project is based on millimeter SMA and APEX observations

with L. E. Kristensen as principal investigator, and near-infrared VLT-ISAAC observations with K. M. Pontoppidan as principal investigator. I carried out the calibration and reduction of the raw SMA and APEX datasets. L. E. Kristensen assisted in this process. The combination of the interferometric and single-dish data was performed by myself and J. K. Jørgensen provided assistance with it. The flux calibration and the telluric absorption line removal of the near-infrared VLT data was performed by K. M. Pontoppidan. The rest of the infrared data reduction, the continuum and optical depth determination, and the spectral decomposition with OMNIFIT was carried out by myself with the assistance of W. R. M. Rocha. Guidance in the usage of OMNIFIT and in the selection of the methodology to derive the column density of the ice species was provided by H. J. Fraser and W. R. Rocha. The ice laboratory components were supplied by H. J. Fraser and prepared to be imported to OMNIFIT by W. R. Rocha. I led the analysis of the millimeter and infrared data and the final discussion. I wrote the paper on my own and made all the figures and tables, except for Figure 5.6 which was made by W. R. Rocha. All co-authors gave valuable inputs and edited the article.

Article II This study makes use of SMA and APEX observations of which I am the principal investigator, and literature ice column densities derived from data taken with the AKARI satellite provided by A. N. Suutarinen. I was actively involved in the SMA data collection. Reduced IRAM 30m maps of the CO isotopologues were obtained from H. J. Fraser group members. The calibration, reduction and combination of the interferometric and single-dish data was performed by myself. L. E. Kristensen assisted with the imaging of the SMA data and J. K. Jørgensen gave valuable inputs for the combination of SMA and APEX data. W. R. Rocha gave support with the production of the H_2 column density map from the visual extinction in the J-band. I led the analysis of the data and the resulting discussion. I wrote the entire paper by myself and created all the tables and figures, except for Figure 1 which was made by K. M. Pontoppidan. P. Bjerkeli supplied important comments during the analysis of the data. All the co-authors made useful suggestions and edited the article.

Article III This paper is based on SMA observations of which I am the principal investigator and literature gas and ice column densities determined from data taken with SMA, APEX and *Spitzer Space telescope* observations. The raw SMA data were calibrated and imaged by myself. I wrote the paper on my own and produced all the tables and figures, except for Figure 1 which was made by W. R. Rocha. We are currently awaiting for the second awarded track of the SMA data, delayed due to the pandemic, which will target the CH_3OH $J = 5 - 4$ branch at 241.791 GHz. The SMA has resumed operations, and our track is supposed to be carried out in the current observational semester. Afterwards, we will be able to combine these SMA data with awarded APEX and ACA data, and to compare the CH_3OH gas-to-ice ratios obtained from literature data with the value calculated from the new SMA data at a higher angular resolution.

Bibliography

1. ALMA Partnership *et al.*, *ApJ* **808**, L3 (2015).
2. K. Acharyya *et al.*, *A&A* **466**, 1005–1012 (2007).
3. C. M. O. D. Alexander *et al.*, *Geochim. Cosmochim. Acta* **71**, 4380–4403 (2007).
4. V. Allen, M. Cordiner, S. Charnley, *arXiv e-prints* (2020).
5. K. Altwegg *et al.*, *Science Advances* **2**, e1600285–e1600285 (2016).
6. F. O. Alves *et al.*, *ApJ* **904**, L6 (2020).
7. J. Alves, M. Lombardi, C. J. Lada, *A&A* **565**, A18 (2014).
8. S. Andersson, E. F. van Dishoeck, *A&A* **491**, 907–916 (2008).
9. S. Andersson *et al.*, *J. Chem. Phys.* **124**, 064715–064715 (2006).
10. D. P. P. Andrade, M. L. M. Rocco, H. M. Boechat-Roberty, *MNRAS* **409**, 1289–1296 (2010).
11. P. André *et al.*, in *Protostars and Planets VI* (Beuther, Henrik et al., 2014), p. 27.
12. P. André *et al.*, *A&A* **518**, L102 (2010).
13. P. André, *Comptes Rendus Geoscience* **349**, 187–197 (2017).
14. P. Andre, D. Ward-Thompson, M. Barsony, *ApJ* **406**, 122 (1993).
15. S. M. Andrews *et al.*, *ApJ* **869**, L41 (2018).
16. M. Ansdell *et al.*, *AJ* **160**, 248 (Dec. 2020).
17. M. Antiñolo *et al.*, *ApJ* **823**, 25 (2016).
18. E. Artur de la Villarmois *et al.*, *A&A* **626**, A71 (2019).
19. C. R. Arumainayagam *et al.*, *Chemical Society Reviews* **48**, 2293–2314 (2019).
20. Y. Aso *et al.*, *ApJ* **863**, 19 (2018).
21. R. Bachiller *et al.*, *A&A* **295**, L51 (1995).
22. R. Bachiller *et al.*, *A&A* **335**, 266–276 (1998).
23. J. Bally, in *Handbook of Star Forming Regions, Volume I* (Reipurth, B., 2008), vol. 4, p. 459.
24. N. Balucani, C. Ceccarelli, V. Taquet, *MNRAS* **449**, L16–L20 (2015).
25. P. J. Barnes *et al.*, *ApJ* **812**, 6 (2015).
26. D. Barrado *et al.*, *A&A* **526**, A21 (2011).
27. D. Barrado *et al.*, *A&A* **612**, A79 (2018).
28. R. Basalgète *et al.*, *A&A* **647**, A35 (2021).
29. R. Basalgète *et al.*, *A&A* **647**, A36 (2021).
30. M. R. Bate, *MNRAS* **475**, 5618–5658 (2018).
31. A. Bayo *et al.*, *A&A* **536**, A63 (2011).
32. C. P. M. Bell *et al.*, *MNRAS* **434**, 806–831 (2013).
33. C. J. Bennett *et al.*, *ApJ* **660**, 1588–1608 (2007).
34. P. J. Benson, P. C. Myers, *ApJS* **71**, 89 (1989).
35. E. A. Bergin, M. Tafalla, *ARA&A* **45**, 339–396 (2007).
36. J. B. Bergner *et al.*, *ApJ* **841**, 120 (2017).
37. J. B. Bergner *et al.*, *ACS Earth and Space Chemistry* **3**, 1564–1575 (2019).
38. M. Bertin *et al.*, *ApJ* **817**, L12 (2016).
39. E. A. Bibo, P. S. The, D. N. Dawanas, *A&A* **260**, 293–302 (1992).
40. S. E. Bisschop *et al.*, *A&A* **449**, 1297–1309 (2006).
41. L. Bizzocchi *et al.*, *A&A* **569**, A27 (2014).

42. P. Bjerkeli *et al.*, *A&A* **546**, A29 (2012).
43. P. Bjerkeli *et al.*, *A&A* **595**, A39 (2016).
44. R. D. Blandford, D. G. Payne, *MNRAS* **199**, 883–903 (1982).
45. S Blanksby, G Ellison, *Accounts of Chemical Research* **36**, 255–263 (2003).
46. J. Blum, G. Wurm, *ARA&A* **46**, 21–56 (2008).
47. D. Bockelee-Morvan *et al.*, *A&A* **287**, 647–665 (1994).
48. C. F. Bohren, D. R. Huffman, *Absorption and scattering of light by small particles* (New York: Wiley, 1983).
49. A. S. Bolina, W. A. Brown, *Surface Science* **598**, 45–56 (2005).
50. W. B. Bonnor, *ZAp* **39**, 143 (1956).
51. S. Bontemps *et al.*, *A&A* **518**, L85 (2010).
52. A. C. A. Boogert, P. A. Gerakines, D. C. B. Whittet, *ARA&A* **53**, 541–581 (2015).
53. A. C. A. Boogert *et al.*, *A&A* **360**, 683–698 (2000).
54. A. C. A. Boogert *et al.*, *ApJ* **678**, 985–1004 (2008).
55. A. C. A. Boogert *et al.*, *ApJ* **729**, 92 (2011).
56. A. C. A. Boogert *et al.*, *ApJ* **777**, 73 (2013).
57. S. Bottinelli *et al.*, *ApJ* **718**, 1100–1117 (2010).
58. F. Brauer, T. Henning, C. P. Dullemond, *A&A* **487**, L1–L4 (2008).
59. D. Bresnahan *et al.*, *A&A* **615**, A125 (2018).
60. D. S. Briggs, F. R. Schwab, R. A. Sramek, in *Synthesis Imaging in Radio Astronomy II* (Taylor, G. B., Carilli, C. L., and Perley, R. A., 1999), vol. 180, p. 127.
61. T. Y. Brooke, K. Sellgren, T. R. Geballe, *ApJ* **517**, 883–900 (1999).
62. A. Brown, *ApJ* **322**, L31 (1987).
63. V. Buch, R. Czerminski, *J. Chem. Phys.* **95**, 6026–6038 (1991).
64. J. V. Buckle *et al.*, *MNRAS* **399**, 1026–1043 (2009).
65. J. V. Buckle *et al.*, *MNRAS* **422**, 521–541 (2012).
66. J. A. Caballero, *A&A* **478**, 667–674 (2008).
67. H. Calcutt *et al.*, *A&A* **616**, A90 (2018).
68. L. Cambrésy, *A&A* **345**, 965–976 (1999).
69. J. A. Cardelli, G. C. Clayton, J. S. Mathis, *ApJ* **345**, 245 (1989).
70. P. Carlhoff *et al.*, *A&A* **560**, A24 (2013).
71. J. M. Carpenter, *AJ* **120**, 3139–3161 (2000).
72. M. M. Casali, C. Eiroa, W. D. Duncan, *A&A* **275**, 195–200 (1993).
73. S. Cazaux *et al.*, *ApJ* **593**, L51–L55 (2003).
74. S. Cazaux *et al.*, *A&A* **585**, A55 (2016).
75. S. Cazaux *et al.*, *ApJ* **849**, 80 (2017).
76. P. Cazzoletti *et al.*, *A&A* **626**, A11 (2019).
77. C. J. Chandler, J. E. Carlstrom, *ApJ* **466**, 338 (1996).
78. N. L. Chapman *et al.*, *ApJ* **690**, 496–511 (2009).
79. S. B. Charnley, A. G. G. M. Tielens, S. D. Rodgers, *ApJ* **482**, L203–L206 (1997).
80. S. B. Charnley, in *IAU Colloq. 161: Astronomical and Biochemical Origins and the Search for Life in the Universe* (Batalli Cosmovici, Cristiano, Bowyer, Stuart, and Werthimer, Dan, 1997), p. 89.
81. H. Chen *et al.*, *ApJ* **445**, 377 (1995).
82. X. Chen, H. G. Arce, *ApJ* **720**, L169–L173 (2010).
83. J. E. Chiar *et al.*, *ApJ* **426**, 240 (1994).
84. J. E. Chiar *et al.*, *ApJ* **570**, 198–209 (2002).
85. J. E. Chiar *et al.*, *ApJ* **731**, 9 (2011).

86. M. Choi, *ApJ* **705**, 1730–1734 (2009).
87. L. E. U. Chu, K. Hodapp, A. Boogert, *ApJ* **904**, 86 (2020).
88. K. J. Chuang *et al.*, *MNRAS* **455**, 1702–1712 (2016).
89. K. J. Chuang *et al.*, *MNRAS* **467**, 2552–2565 (2017).
90. A. Ciaravella *et al.*, *Proceedings of the National Academy of Science* **117**, 16149–16153 (2020).
91. M. P. Collings *et al.*, *ApJ* **583**, 1058–1062 (2003).
92. M. P. Collings *et al.*, *MNRAS* **354**, 1133–1140 (2004).
93. M. S. Connelley, B. Reipurth, A. T. Tokunaga, *AJ* **135**, 2496–2525 (2008).
94. P. S. Conti, E. M. Leep, *ApJ* **193**, 113–124 (1974).
95. A. M. Craigon, http://digitool.lib.strath.ac.uk/R/?func=dbin-jump-full&object_id=27550, PhD thesis, Dept. of Physics, Univ. of Strathclyde, 2015.
96. G. A. Cruz-Diaz *et al.*, *A&A* **592**, A68 (2016).
97. H. M. Cuppen, E. Herbst, *ApJ* **668**, 294–309 (2007).
98. H. M. Cuppen *et al.*, *MNRAS* **417**, 2809–2816 (2011).
99. H. M. Cuppen *et al.*, *Space Sci. Rev.* **212**, 1–58 (2017).
100. A. Dalgarno, in, ed. by B. Bederson, A. Dalgarno (Academic Press, 1994), vol. 32, pp. 57–68.
101. T. M. Dame, P. Thaddeus, *ApJ* **297**, 751–765 (1985).
102. T. M. Dame *et al.*, *ApJ* **322**, 706 (1987).
103. E. Dartois *et al.*, *A&A* **618**, A173 (2018).
104. E. Dartois *et al.*, *Astronomy and Astrophysics* **627**, A55 (2019).
105. E. Dartois *et al.*, *A&A* **634**, A103 (2020).
106. A. Das *et al.*, *ApJS* **237**, 9 (2018).
107. C. J. Davis *et al.*, *MNRAS* **309**, 141–152 (1999).
108. A. Dawes, N. J. Mason, H. J. Fraser, *Phys. Chem. Chem. Phys.* **18**, 1245–1257 (2 2016).
109. C. H. De Vries, G. Narayanan, R. L. Snell, *ApJ* **577**, 798–825 (2002).
110. J. T. Dempsey *et al.*, *MNRAS* **430**, 2534–2544 (2013).
111. J. P. Devlin, *J. Chem. Phys* **96**, 6185–6188 (1992).
112. J. Di Francesco *et al.*, *ApJS* **175**, 277–295 (2008).
113. S. Dib, T. Henning, *A&A* **629**, A135 (2019).
114. O. Dionatos *et al.*, *A&A* **558**, A88 (2013).
115. O. Dionatos *et al.*, *A&A* **563**, A28 (2014).
116. C. J. Dolan, R. D. Mathieu, *AJ* **118**, 2409–2423 (1999).
117. C. J. Dolan, R. D. Mathieu, *AJ* **123**, 387–403 (2002).
118. B. T. Draine, *ARA&A* **41**, 241–289 (2003).
119. B. T. Draine, F. Bertoldi, *ApJ* **468**, 269 (1996).
120. M. N. Drozdovskaya *et al.*, *MNRAS* **490**, 50–79 (2019).
121. A. Duarte-Cabral *et al.*, *A&A* **519**, A27 (2010).
122. F. Dulieu *et al.*, *Scientific Reports* **3**, 1338 (2013).
123. M. M. Dunham *et al.*, in *Protostars and Planets VI* (Beuther, Henrik et al., 2014), p. 195.
124. M. M. Dunham *et al.*, *ApJS* **220**, 11 (2015).
125. R. Dupuy *et al.*, *Nature Astronomy* **2**, 796–801 (2018).
126. A. Duquennoy, M. Mayor, *A&A* **500**, 337–376 (1991).
127. R. Ebert, *ZAp* **37**, 217 (1955).
128. P. Ehrenfreund, S. B. Charnley, *ARA&A* **38**, 427–483 (2000).
129. C. Eiroa, M. M. Casali, *A&A* **223**, L17–L19 (1989).

130. C. Eiroa, A. A. Djupvik, M. M. Casali, in *Handbook of Star Forming Regions, Volume II: The Southern Sky ASP Monograph Publications* (Reipurth, B. ed, 2008), vol. 5, p. 693.
131. C. Eistrup, C. Walsh, E. F. van Dishoeck, *A&A* **595**, A83 (2016).
132. D. D. Eley, E. K. Rideal, *Nature* **146**, 401–402 (1940).
133. I. Evans Neal J. *et al.*, *ApJS* **181**, 321–350 (2009).
134. N. J. Evans II *et al.*, *VizieR Online Data Catalog* **2332** (2014).
135. E. C. Fayolle *et al.*, *ApJ* **739**, L36 (2011).
136. E. C. Fayolle *et al.*, *ApJ* **816**, L28 (2016).
137. G. G. Fazio *et al.*, *ApJS* **154**, 10–17 (2004).
138. G. Fedoseev *et al.*, *MNRAS* **448**, 1288–1297 (2015).
139. G. Fedoseev *et al.*, *MNRAS* **446**, 439–448 (2015).
140. G. Fedoseev *et al.*, *ApJ* **842**, 52 (2017).
141. S. Ferrero *et al.*, *ApJ* **904**, 11 (2020).
142. J. Forbrich, T. Preibisch, *A&A* **475**, 959–972 (2007).
143. J. Forbrich *et al.*, *A&A* **464**, 1003–1013 (2007).
144. D. Foreman-Mackey *et al.*, *PASP* **125**, 306 (2013).
145. H. J. Fraser, E. F. van Dishoeck, *Advances in Space Research* **33**, 14–22 (2004).
146. H. J. Fraser *et al.*, *MNRAS* **327**, 1165–1172 (2001).
147. H. J. Fraser *et al.*, *MNRAS* **353**, 59–68 (2004).
148. S. Frimann, J. K. Jørgensen, T. Haugbølle, *A&A* **587**, A59 (2016).
149. G. W. Fuchs *et al.*, *A&A* **505**, 629–639 (2009).
150. P. A. B. Galli *et al.*, *A&A* **634**, A98 (2020).
151. R. T. Garrod, E. Herbst, *A&A* **457**, 927–936 (2006).
152. R. T. Garrod, V. Wakelam, E. Herbst, *A&A* **467**, 1103–1115 (2007).
153. R. T. Garrod, S. L. Widicus Weaver, E. Herbst, *ApJ* **682**, 283–302 (2008).
154. W. D. Geppert *et al.*, *Faraday Discussions* **133**, 177 (2006).
155. P. A. Gerakines *et al.*, *A&A* **296**, 810 (1995).
156. G. Giardino *et al.*, *A&A* **463**, 275–288 (2007).
157. E. L. Gibb *et al.*, *ApJS* **151**, 35–73 (2004).
158. B. M. Giuliano *et al.*, *A&A* **592**, A81 (2016).
159. P. F. Goldsmith, W. D. Langer, *ApJ* **517**, 209–225 (1999).
160. M. Goto *et al.*, *arXiv e-prints* (2020).
161. R. J. Gould, E. E. Salpeter, *ApJ* **138**, 393 (1963).
162. L. V. Gramajo *et al.*, *AJ* **139**, 2504–2524 (2010).
163. T. Grassi *et al.*, *A&A* **643**, A155 (Nov. 2020).
164. R. O. Gray *et al.*, *AJ* **132**, 161–170 (2006).
165. G. M. Green *et al.*, *ApJ* **810**, 25 (2015).
166. M. J. Griffin *et al.*, *A&A* **518**, L3 (2010).
167. R. J. A. Grim *et al.*, *A&A* **243**, 473 (1991).
168. C. E. Groppi *et al.*, *ApJ* **670**, 489–498 (2007).
169. W. M. Grundy *et al.*, *Science* **367**, aay3705 (2020).
170. R. Güsten *et al.*, *A&A* **454**, L13–L16 (2006).
171. R. A. Gutermuth *et al.*, *ApJ* **673**, L151 (2008).
172. W. Hagen, L. J. Allamandola, J. M. Greenberg, *A&A* **86**, L3–L6 (1980).
173. G. Haro, *ApJ* **115**, 572 (1952).

174. J. Harris, B. Kasemo, *Surface Science* **105**, L281–L287 (1981).
175. D. Harsono *et al.*, *A&A* **562**, A77 (2014).
176. D. Harsono *et al.*, *Nature Astronomy* **2**, 646–651 (2018).
177. P. Hartigan, J. A. Graham, *AJ* **93**, 913 (1987).
178. P. Harvey *et al.*, *ApJ* **663**, 1149–1173 (2007).
179. T. I. Hasegawa, E. Herbst, *MNRAS* **263**, 589 (1993).
180. T. I. Hasegawa, E. Herbst, C. M. Leung, *ApJS* **82**, 167 (1992).
181. T. Hassenkam *et al.*, *Nature* **548**, 78–81 (2017).
182. T. J. Haworth *et al.*, *MNRAS* **501**, 3502–3514 (2021).
183. C. Heiles, H. J. Habing, *A&AS* **14**, 1 (1974).
184. T. T. Helfer *et al.*, *ApJS* **145**, 259–327 (2003).
185. T. Henning, *ARA&A* **48**, 21–46 (2010).
186. T. Henning, G. Meeus, in *Physical Processes in Circumstellar Disks around Young Stars* (Garcia, Paulo J. V., 2011), pp. 114–148.
187. G. H. Herbig, *Vistas in Astronomy* **8**, 109–125 (1966).
188. G. H. Herbig, *ApJ* **111**, 11 (1950).
189. G. H. Herbig, *ApJS* **4**, 337 (1960).
190. E. Herbst, W. Klemperer, *ApJ* **185**, 505–534 (1973).
191. E. Herbst, C. M. Leung, *ApJS* **69**, 271 (1989).
192. E. Herbst, E. F. van Dishoeck, *ARA&A* **47**, 427–480 (2009).
193. G. J. Herczeg *et al.*, *ApJ* **849**, 43 (2017).
194. G. J. Herczeg *et al.*, *ApJ* **878**, 111 (2019).
195. J. Hernández *et al.*, *ApJ* **662**, 1067–1081 (2007).
196. J. Hernández *et al.*, *ApJ* **707**, 705–715 (2009).
197. J. Hernández *et al.*, *ApJ* **794**, 36 (2014).
198. M. Heyer, T. M. Dame, *ARA&A* **53**, 583–629 (2015).
199. C. N. Hinshelwood, in (Oxford University Press, 1940), pp. 36–39.
200. P. T. P. Ho, J. M. Moran, K. Y. Lo, *ApJ* **616**, L1–L6 (2004).
201. S. Hoban *et al.*, *Icarus* **105**, 548–556 (1993).
202. J. A. Högbom, *A&AS* **15**, 417 (1974).
203. D. J. Hollenbach, A. G. G. M. Tielens, *Reviews of Modern Physics* **71**, 173–230 (1999).
204. D. Hollenbach, C. F. McKee, *ApJ* **342**, 306 (1989).
205. D. Hollenbach, E. E. Salpeter, *ApJ* **163**, 155 (1971).
206. M. Honda *et al.*, *ApJ* **690**, L110–L113 (2009).
207. D. M. Hudgins *et al.*, *ApJS* **86**, 713–870 (1993).
208. C. L. H. Hull *et al.*, *ApJ* **847**, 92 (2017).
209. R. L. Hurt, M. Barsony, *ApJ* **460**, L45 (1996).
210. S. Ioppolo *et al.*, *ApJ* **686**, 1474–1479 (2008).
211. S. Ioppolo *et al.*, *MNRAS* **413**, 2281–2287 (2011).
212. S. Ioppolo *et al.*, *A&A* **646**, A172 (2021).
213. M. Ishii *et al.*, *AJ* **124**, 2790–2798 (2002).
214. J. H. Jeans, *Philosophical Transactions of the Royal Society of London Series A* **199**, 1–53 (1902).
215. R. D. Jeffries, *MNRAS* **376**, 1109–1119 (2007).
216. A. Jiménez-Escobar *et al.*, *ApJ* **820**, 25 (2016).
217. A. Jiménez-Escobar *et al.*, *ApJ* **868**, 73 (2018).

218. I. Jiménez-Serra *et al.*, *A&A* **482**, 549–559 (2008).
219. I. Jiménez-Serra *et al.*, *Astrobiology* **20**, 1048–1066 (2020).
220. D. Johnstone *et al.*, *ApJ* **559**, 307–317 (2001).
221. J. K. Jørgensen *et al.*, *A&A* **415**, 1021–1037 (2004).
222. J. K. Jørgensen *et al.*, *A&A* **595**, A117 (2016).
223. J. K. Jørgensen, A. Belloche, R. T. Garrod, *ARA&A* **58**, 727–778 (2020).
224. G. Jungclaus *et al.*, *Meteoritics* **11**, 231–237 (1976).
225. J. Kauffmann *et al.*, *A&A* **487**, 993–1017 (2008).
226. J. V. Keane *et al.*, *A&A* **376**, 254–270 (2001).
227. M. Keppler *et al.*, *A&A* **617**, A44 (2018).
228. G. Kim *et al.*, *ApJS* **249**, 33 (2020).
229. R. F. Knacke *et al.*, *ApJ* **179**, 847–854 (1973).
230. C. Knez *et al.*, *ApJ* **635**, L145–L148 (2005).
231. J. Koda *et al.*, *ApJS* **193**, 19 (2011).
232. K. W. Kolasinski, in (Wiley, J. & Sons Ltd., Chichester, England, 1st Ed., 2002).
233. V. Könyves *et al.*, *A&A* **584**, A91 (2015).
234. M. Kounkel, *ApJ* **902**, 122 (2020).
235. M. Kounkel *et al.*, *AJ* **156**, 84 (2018).
236. L. E. Kristensen, M. M. Dunham, *A&A* **618**, A158 (2018).
237. L. E. Kristensen *et al.*, *A&A* **516**, A57 (2010).
238. M. Kuffmeier, B. Zhao, P. Caselli, *A&A* **639**, A86 (2020).
239. M. Kuffmeier, T. Haugbølle, Å. Nordlund, *ApJ* **846**, 7 (2017).
240. Y. Kurono, K.-I. Morita, T. Kamazaki, *PASJ* **61**, 873 (2009).
241. C. J. Lada, J. H. Black, *ApJ* **203**, L75–L79 (1976).
242. C. J. Lada, in *Star Forming Regions* (Peimbert, Manuel and Jugaku, Jun, 1987), vol. 115, p. 1.
243. E. F. Ladd, G. A. Fuller, J. R. Deane, *ApJ* **495**, 871–890 (1998).
244. W. J. Lang *et al.*, *A&A* **357**, 1001–1012 (2000).
245. P. Langevin, *J. Phys. Theor. Appl.* **4**, 678 (1905).
246. I. Langmuir, *Trans. Faraday Soc.* **17**, 607–620 (1922).
247. B. Larsson *et al.*, *A&A* **363**, 253–268 (2000).
248. L. Le Roy *et al.*, *A&A* **583**, A1 (2015).
249. H. H. Lee *et al.*, *A&A* **311**, 690–707 (1996).
250. H.-T. Lee *et al.*, *ApJ* **624**, 808–820 (2005).
251. K. I. Lee *et al.*, *ApJ* **797**, 76 (2014).
252. K. Levenberg, *Quart. Appl. Math.* **2**, 164–168 (1944).
253. Y. Lin *et al.*, *ApJ* **840**, 22 (2017).
254. J. E. Lindberg, J. K. Jørgensen, *A&A* **548**, A24 (2012).
255. J. E. Lindberg *et al.*, *A&A* **584**, A28 (2015).
256. J. E. Lindberg *et al.*, *A&A* **566**, A74 (2014).
257. J. E. Lindberg *et al.*, *ApJ* **835**, 3 (2017).
258. H. Linnartz, S. Ioppolo, G. Fedoseev, *International Reviews in Physical Chemistry* **34**, 205–237 (2015).
259. T. Liu *et al.*, *ApJS* **222**, 7 (2016).
260. R. Lüst, A. Schlüter, *ZAp* **38**, 190 (1955).
261. M.-M. Mac Low, R. S. Klessen, *Reviews of Modern Physics* **76**, 125–194 (2004).
262. R. J. Maddalena, M. Morris, *ApJ* **323**, 179 (1987).

263. E. E. Mamajek, in *Exoplanets and Disks: Their Formation and Diversity* (Usuda, Tomonori, Tamura, Motohide, and Ishii, Miki, 2009), vol. 1158, pp. 3–10.

264. E. E. Mamajek, M. R. Meyer, J. Liebert, *AJ* **124**, 1670–1694 (2002).

265. S. Manigand *et al.*, *A&A* **635**, A48 (2020).

266. D. Marquardt, *J. Soc. Indust. Appl. Math.* **11**, 431–441 (1963).

267. R. Martín-Doménech, G. M. Muñoz Caro, G. A. Cruz-Díaz, *A&A* **589**, A107 (2016).

268. R. Martín-Doménech *et al.*, *ApJ* **880**, 130 (2019).

269. R. D. Mathieu, in *in Handbook of Star Forming Regions, Volume I. The Northern Sky* (Reipurth, B. ed, 2008), vol. 4, ASP Monographs, p. 757.

270. A. J. Maury *et al.*, *A&A* **621**, A76 (2019).

271. B. A. McGuire, *ApJS* **239**, 17 (2018).

272. J. P. McMullin *et al.*, in *Astronomical Data Analysis Software and Systems XVI* (Shaw, R. A., Hill, F., and Bell, D. J., 2007), vol. 376, p. 127.

273. J. P. McMullin *et al.*, *ApJ* **424**, 222 (1994).

274. J. P. McMullin *et al.*, *ApJ* **536**, 845–856 (2000).

275. S. T. Megeath *et al.*, *AJ* **144**, 192 (2012).

276. S. T. Megeath *et al.*, *AJ* **151**, 5 (2016).

277. C. Meinert *et al.*, *Science* **352**, 208–212 (2016).

278. K. M. Menten *et al.*, *A&A* **474**, 515–520 (2007).

279. D. Mesa *et al.*, *A&A* **624**, A4 (2019).

280. L. Mestel, *MNRAS* **138**, 359 (1968).

281. O. Miettinen *et al.*, *A&A* **486**, 799–806 (2008).

282. M. Minissale *et al.*, *A&A* **585**, A24 (2016).

283. M. Minissale *et al.*, *MNRAS* **458**, 2953–2961 (2016).

284. N. Miyauchi *et al.*, *Chemical Physics Letters* **456**, 27–30 (2008).

285. P. Modica, M. E. Palumbo, G. Strazzulla, *Planet. Space Sci.* **73**, 425–429 (2012).

286. S. J. Mojzsis *et al.*, *Nature* **384**, 55–59 (1996).

287. L. K. Morgan *et al.*, *A&A* **477**, 557–571 (2008).

288. J. C. Mottram *et al.*, *A&A* **600**, A99 (2017).

289. J. Moultaka *et al.*, *A&A* **425**, 529–542 (2004).

290. G. M. Muñoz Caro *et al.*, *ACS Earth and Space Chemistry* **3**, 2138–2157 (2019).

291. H. S. P. Müller *et al.*, *A&A* **370**, L49–L52 (2001).

292. M. J. Mumma, S. B. Charnley, *ARA&A* **49**, 471–524 (2011).

293. K. Murakawa, M. Tamura, T. Nagata, *ApJS* **128**, 603–613 (2000).

294. P. Murdin, M. V. Penston, *MNRAS* **181**, 657 (1977).

295. N. M. Murillo *et al.*, *A&A* **592**, A56 (2016).

296. P. C. Myers, E. F. Ladd, *ApJ* **413**, L47 (1993).

297. P. C. Myers, R. A. Linke, P. J. Benson, *ApJ* **264**, 517–537 (1983).

298. P. C. Myers *et al.*, *ApJ* **324**, 907 (1988).

299. P. C. Myers, *ApJ* **700**, 1609–1625 (2009).

300. F. Nakamura *et al.*, *ApJ* **837**, 154 (2017).

301. J. Nelder, R. Mead, *The Computer Journal* **7**, 308 (1965).

302. D. A. Neufeld, A. Dalgarno, *ApJ* **340**, 869 (1989).

303. R. Neuhäuser, J. Forbrich, in *Handbook of Star Forming Regions, Volume II* (Reipurth, B., 2008), vol. 5, p. 735.

304. R. Neuhäuser *et al.*, *A&AS* **146**, 323–347 (2000).

305. B. Nisini *et al.*, *A&A* **518**, L120 (2010).

306. J. A. Noble *et al.*, *MNRAS* **421**, 768–779 (2012).
307. J. A. Noble *et al.*, *ApJ* **775**, 85 (2013).
308. J. A. Noble *et al.*, *Monthly Notices of the Royal Astronomical Society* **467**, 4753–4762 (2017).
309. J. A. Noble, PhD thesis, Dept. of Physics, Univ. of Strathclyde, 2011.
310. M. Nuevo, G. Cooper, S. A. Sandford, *Nature Communications* **9**, 5276 (2018).
311. D. J. Nutter, D. Ward-Thompson, P. André, *MNRAS* **357**, 975–982 (2005).
312. K. I. Öberg, S. Bottinelli, E. F. van Dishoeck, *A&A* **494**, L13–L16 (2009).
313. K. I. Öberg *et al.*, *ApJ* **621**, L33–L36 (2005).
314. K. I. Öberg *et al.*, *A&A* **504**, 891–913 (2009).
315. K. I. Öberg *et al.*, *ApJ* **740**, 109 (2011).
316. K. I. Öberg, *Chemical Reviews* **116**, 9631–9663 (2016).
317. K. I. Öberg, E. A. Bergin, *Phys. Rep.* **893**, 1–48 (2021).
318. K. I. Öberg, R. Murray-Clay, E. A. Bergin, *ApJ* **743**, L16 (2011).
319. K. I. Öberg *et al.*, *ApJ* **740**, 14 (2011).
320. T. Oka, *Proceedings of the National Academy of Science* **103**, 12235–12242 (2006).
321. G. N. Ortiz-León *et al.*, *ApJ* **869**, L33 (2018).
322. V. Ossenkopf, T. Henning, *A&A* **291**, 943–959 (1994).
323. P. Padoan, Å. Nordlund, *ApJ* **576**, 870–879 (2002).
324. Y. J. Pendleton, A. G. G. M. Tielens, M. W. Werner, *ApJ* **349**, 107 (1990).
325. E. M. Penteado, C. Walsh, H. M. Cuppen, *ApJ* **844**, 71 (2017).
326. G. Perotti *et al.*, *A&A* **643**, A48 (2020).
327. G. Perotti *et al.*, *A&A* **650**, A168 (2021).
328. D. E. Peterson *et al.*, *ApJS* **194**, 43 (2011).
329. H. M. Pickett *et al.*, *J. Quant. Spectr. Rad. Transf.* **60**, 883–890 (1998).
330. J. B. Pickles, D. A. Williams, *Ap&SS* **52**, 443–452 (1977).
331. M. Planck, *Verhandl. Dtsch. phys. Ges.* **2**, 202 (1900).
332. D. Polychroni *et al.*, *ApJ* **777**, L33 (2013).
333. K. M. Pontoppidan, *A&A* **453**, L47–L50 (2006).
334. K. M. Pontoppidan, S. M. Blevins, *Faraday Discussions* **168**, 49–60 (2014).
335. K. M. Pontoppidan, E. F. van Dishoeck, E. Dartois, *A&A* **426**, 925–940 (2004).
336. K. M. Pontoppidan *et al.*, *A&A* **408**, 981–1007 (2003).
337. K. M. Pontoppidan *et al.*, *A&A* **404**, L17–L20 (2003).
338. K. M. Pontoppidan *et al.*, *ApJ* **678**, 1005–1031 (2008).
339. K. M. Pontoppidan *et al.*, in *Protostars and Planets VI* (Beuther, Henrik et al., 2014), p. 363.
340. K. M. Pontoppidan *et al.*, *ApJ* **874**, 92 (2019).
341. M. S. Povich *et al.*, *ApJS* **209**, 31 (2013).
342. T. Preibisch, *A&A* **410**, 951–959 (2003).
343. T. Preibisch, *A&A* **428**, 569–577 (2004).
344. R. E. Pudritz, T. P. Ray, *Frontiers in Astronomy and Space Sciences* **6**, 54 (2019).
345. D. Qasim *et al.*, *A&A* **612**, A83 (2018).
346. D. Qasim *et al.*, *Nature Astronomy* **4**, 781–785 (2020).
347. S.-L. Qin, Y.-F. Wu, *Chinese J. Astron. Astrophys.* **3**, 69–74 (2003).
348. D. Rabli, D. R. Flower, *MNRAS* **406**, 95–101 (2010).
349. F. R. S. Rayleigh, *XXXI. Investigations in optics, with special reference to the spectroscope*, 1879.
350. P. Redondo, C. Barrientos, A. Largo, *ApJ* **836**, 240 (2017).

351. P. Redondo *et al.*, *A&A* **603**, A139 (2017).
352. B. Reipurth, *VizieR Online Data Catalog*, V/104 (2000).
353. B. Reipurth, J. Bally, *ARA&A* **39**, 403–455 (2001).
354. B. Reipurth, P. Friberg, *MNRAS* **501**, 5938–5947 (2021).
355. V. M. Rivilla *et al.*, *MNRAS* **483**, L114–L119 (2019).
356. H. Roberts, T. J. Millar, *A&A* **361**, 388–398 (2000).
357. T. P. Robitaille, *A&A* **600**, A11 (2017).
358. T. P. Robitaille *et al.*, *ApJS* **169**, 328–352 (2007).
359. T. P. Robitaille *et al.*, *ApJS* **167**, 256–285 (2006).
360. W. R. M. Rocha, S. Pilling, *ApJ* **803**, 18 (2015).
361. K. Rohlfs, T. L. Wilson, *Tools of Radio Astronomy* (Springer Verlag, 1996).
362. G. S. Rossano, *AJ* **83**, 234–240 (1978).
363. L. S. Rothman *et al.*, *Appl. Opt.* **26**, 4058–4097 (1987).
364. M. Rubin *et al.*, *MNRAS* **489**, 594–607 (2019).
365. D. P. Ruffle, E. Herbst, *MNRAS* **322**, 770–778 (2001).
366. D. P. Ruffle, E. Herbst, *MNRAS* **324**, 1054–1062 (2001).
367. D. Rumble *et al.*, *MNRAS* **448**, 1551–1573 (2015).
368. M. Sahan, L. M. Haffner, *AJ* **151**, 147 (2016).
369. G. Santangelo *et al.*, *A&A* **538**, A45 (2012).
370. S. L. Schnee *et al.*, *ApJ* **634**, 442–450 (2005).
371. S. Schneider, B. G. Elmegreen, *ApJS* **41**, 87–95 (1979).
372. F. L. Schöier *et al.*, *A&A* **390**, 1001–1021 (2002).
373. F. L. Schöier *et al.*, *A&A* **432**, 369–379 (2005).
374. F. L. Schöier *et al.*, *A&A* **454**, L67–L70 (2006).
375. W. A. Schutte *et al.*, *A&A* **343**, 966–976 (1999).
376. D. M. Segura-Cox *et al.*, *ApJ* **866**, 161 (2018).
377. D. M. Segura-Cox *et al.*, *Nature* **586**, 228–231 (2020).
378. R. J. Shannon *et al.*, *Nature Chemistry* **5**, 745–749 (2013).
379. R. J. Shannon *et al.*, *RSC Advances* **4**, 26342–26353 (2014).
380. S. Sharpless, *ApJS* **4**, 257 (1959).
381. T. Shimonishi *et al.*, *ApJ* **855**, 27 (2018).
382. F. H. Shu, *ApJ* **214**, 488–497 (1977).
383. M. A. J. Simons, T. Lamberts, H. M. Cuppen, *A&A* **634**, A52 (2020).
384. D. Skouteris *et al.*, *ApJ* **854**, 135 (2018).
385. M. F. Skrutskie *et al.*, *AJ* **131**, 1163–1183 (2006).
386. L. Song, J. Kästner, *ApJ* **850**, 118 (2017).
387. S. Spezzano *et al.*, *A&A* **643**, A60 (2020).
388. F. Stahler, S. W. Palla, in *The Formation of Stars* (Wiley-VCH Verlag GmbG & Co, 2004).
389. S. Stanimirovic, in *Single-Dish Radio Astronomy: Techniques and Applications* (Stanimirovic, Snezana et al., 2002), vol. 278, pp. 375–396.
390. T. P. Stecher, D. A. Williams, *Astrophys. Lett.* **4**, 99 (1969).
391. D. P. Stevenson, D. O. Schissler, *J. Chem. Phys.* **29**, 282 (1958).
392. S. E. Strom, G. L. Grasdalen, K. M. Strom, *ApJ* **191**, 111–142 (1974).
393. K. Sugitani, Y. Fukui, K. Ogura, *ApJS* **77**, 59 (1991).
394. A. N. Suutarinen *et al.*, *MNRAS* **440**, 1844–1855 (2014).

395. A. Suutarinen, http://oro.open.ac.uk/61309/, PhD thesis, Dept. of Physics, The Open University, 2015.
396. A. Suutarinen, *omnifit v0.1*, https://doi.org/10.5281/zenodo.29354, 2015.
397. K. N. R. Taylor, J. W. V. Storey, *MNRAS* **209**, 5P–10 (1984).
398. S. Terebey, F. H. Shu, P. Cassen, *ApJ* **286**, 529–551 (1984).
399. J. Terwisscha van Scheltinga *et al.*, *A&A* **611**, A35 (2018).
400. W.-F. Thi *et al.*, *A&A* **449**, 251–265 (2006).
401. A. G. G. M. Tielens, W. Hagen, *A&A* **114**, 245–260 (1982).
402. J. J. Tobin *et al.*, *Nature* **492**, 83–85 (2012).
403. J. J. Tobin *et al.*, *ApJ* **805**, 125 (2015).
404. W. Tscharnuter, *A&A* **39**, 207 (1975).
405. B. E. Turner, *ApJ* **501**, 731–748 (1998).
406. Ł. Tychoniec *et al.*, *A&A* **632**, A101 (2019).
407. Ł. Tychoniec *et al.*, *A&A* **640**, A19 (2020).
408. M. Vasta *et al.*, *A&A* **537**, A98 (2012).
409. A. I. Vasyunin, E. Herbst, *ApJ* **769**, 34 (2013).
410. A. I. Vasyunin *et al.*, *ApJ* **842**, 33 (2017).
411. F. Vazart *et al.*, *MNRAS* **499**, 5547–5561 (2020).
412. R. Visser, S. D. Doty, E. F. van Dishoeck, *A&A* **534**, A132 (2011).
413. R. Visser *et al.*, *A&A* **495**, 881–897 (2009).
414. S. N. Vogel *et al.*, *ApJ* **283**, 655–667 (1984).
415. C. M. Wade, *AJ* **62**, 148 (1957).
416. A. F. Wagner, M. M. Graff, *ApJ* **317**, 423 (1987).
417. V. Wakelam *et al.*, *Molecular Astrophysics* **9**, 1–36 (2017).
418. C. Walsh *et al.*, *ApJ* **823**, L10 (2016).
419. F. M. Walter *et al.*, *Mem. Soc. Astron. Italiana* **68**, 1081–1088 (1997).
420. H. Wang *et al.*, *ApJ* **617**, 1191–1203 (2004).
421. N. Watanabe, A. Kouchi, *ApJ* **571**, L173–L176 (2002).
422. Y. Watanabe *et al.*, *ApJ* **745**, 126 (2012).
423. W. D. Watson, E. E. Salpeter, *ApJ* **174**, 321 (1972).
424. W. D. Watson, *ApJ* **183**, L17 (1973).
425. J. C. Weingartner, B. T. Draine, *ApJ* **548**, 296–309 (2001).
426. A. Weiß *et al.*, *A&A* **365**, 571–587 (2001).
427. M. S. Westley *et al.*, *Nature* **373**, 405–407 (1995).
428. G. J. White, M. M. Casali, C. Eiroa, *A&A* **298**, 594 (1995).
429. B. A. Whitney *et al.*, *ApJ* **598**, 1079–1099 (2003).
430. D. C. B. Whittet *et al.*, *ApJ* **742**, 28 (2011).
431. D. A. Williams, S. Viti, *Observational Molecular Astronomy: Exploring the Universe Using Molecular Line Emissions* (Cambridge University Press, 2013).
432. J. P. Williams, W. M. J. Best, *ApJ* **788**, 59 (2014).
433. J. P. Williams, L. A. Cieza, *ARA&A* **49**, 67–117 (2011).
434. T. L. Wilson, *Reports on Progress in Physics* **62**, 143–185 (1999).
435. T. L. Wilson, F. Matteucci, *A&A Rev.* **4**, 1–33 (1992).
436. A. J. Winter *et al.*, *MNRAS* **491**, 903–922 (2020).
437. M. G. Wolfire, D. Hollenbach, A. G. G. M. Tielens, *ApJ* **344**, 770 (1989).
438. E. L. Wright *et al.*, *AJ* **140**, 1868–1881 (2010).

439. B. Yang *et al.*, *ApJ* **718**, 1062–1069 (2010).
440. H.-W. Yi *et al.*, *ApJS* **236**, 51 (2018).
441. H.-W. Yi *et al.*, *arXiv e-prints*, arXiv:2103.03499 (2021).
442. L. Zamirri *et al.*, *MNRAS* **480**, 1427–1444 (2018).
443. G. Zasowski *et al.*, *ApJ* **694**, 459–478 (2009).
444. F. Zernike, *Physica* **5**, 785–795 (1938).
445. C. Y. Zhang *et al.*, *A&A* **218**, 231–240 (1989).
446. C. Zhang *et al.*, *MNRAS* **497**, 793–808 (2020).
447. Z.-Y. Zhang *et al.*, *Nature* **558**, 260–263 (2018).
448. C. Zucker *et al.*, *ApJ* **879**, 125 (2019).
449. C. Zucker *et al.*, *A&A* **633**, A51 (2020).
450. P. H. van Cittert, *Physica* **1**, 201–210 (1934).
451. E. F. van Dishoeck, in *Millimetre and Submillimetre Astronomy* (Wolstencroft, R. D. and Burton, W. B., 1988), vol. 147, p. 117.
452. E. F. van Dishoeck, J. H. Black, *ApJS* **62**, 109 (1986).
453. E. F. van Dishoeck, E. A. Bergin, *arXiv e-prints* (2020).
454. E. F. van Dishoeck, J. H. Black, *ApJ* **334**, 771 (1988).
455. E. F. van Dishoeck, G. A. Blake, *ARA&A* **36**, 317–368 (1998).
456. M. L. van Gelder *et al.*, *A&A* **639**, A87 (2020).
457. S. E. van Terwisga *et al.*, *A&A* **640**, A27 (2020).
458. H. C. van de Hulst, *Recherches Astronomiques de l'Observatoire d'Utrecht* **11**, 2.i–2 (1946).
459. M. L. R. van 't Hoff *et al.*, *A&A* **599**, A101 (2017).
460. M. L. R. van 't Hoff *et al.*, *ApJ* **864**, L23 (2018).